

Journal of Materials and Engineering Structures

Research Paper

Characterization and Performance Evaluation of Thick-film Based Strain Sensors for Structural Health Monitoring Applications

Ivanka Stanimirović [a,*], *Pavle Stanimirović* [b], *Aleksandar Savić* [c], *Zdravko Stanimirović* [a]

[a] *Vinča Institute of Nuclear Sciences – National Institute of the Republic of Serbia, University of Belgrade, Mike Petrovića Alasa 12-14, 11000 Belgrade, Serbia*

[b] *Faculty of Transport and Traffic Engineering, University of Belgrade, Vojvode Stepe 305, 11000 Belgrade, Serbia*

[c] *Faculty of Civil Engineering, University of Belgrade, Bulevar kralja Aleksandra 73, 11000 Belgrade, Serbia*

ARTICLE INFO

Article history :

Received : 5 December 2025

Revised : 24 February 2026

Accepted : 28 February 2026

Keywords:

Sintered thick resistive film

Structural health monitoring

Strain-sensing technology

Steel constructions

ABSTRACT

This paper investigates the use of sintered thick resistive films as strain sensors for the health monitoring of structural components commonly encountered in modern civil engineering applications. A series of thick-film strain sensors was developed and tested to assess their feasibility for integration with steel bars. The sensors were fabricated by combining a Pd/Ag conductive composition with a thick resistive film based on bismuth-ruthenate, which was deposited and sintered on alumina ceramic substrates. The sensors underwent a three-point bending test in their freestanding form, while a four-point bending test was conducted on sensors adhered to the upper surface of steel bars to simulate real-world conditions. Under mechanical strain, reversible deformations in the sensor were detected as changes in the resistivity of the thick resistive film. The performance of the sensors was evaluated through a series of tests, including resistance measurements, gauge factor calculations, temperature stability analysis and high-voltage surge testing. These evaluations provide valuable insights into the suitability of thick-film sensors for structural health monitoring in civil engineering, particularly in relation to steel constructions.

1 Introduction

During their service life, civil engineering structures are subjected to progressive aging and various environmental stressors, including seismic activity, hydrodynamic forces, soil displacement and extreme weather conditions. The increasing complexity and scale of modern infrastructure necessitate the development and implementation of advanced Structural Health Monitoring (SHM) systems to ensure structural integrity, improve safety and optimize maintenance strategies. SHM is based on the premise that the mechanical and material properties of a structure evolve due to external loads, fatigue, corrosion and other degradation mechanisms. By continuously monitoring strain variations, internal stresses and other key indicators, it is possible to detect early signs of structural damage and predict failure before catastrophic events occur [1-4]. Strain

* *Corresponding author. Tel.: +381642020134.*
E-mail address: ivanka.stanimirovic@vin.bg.ac.rs

e-ISSN: 2170-127X, (cc) BY-SA

RESEARCH REVIEW of Sciences and Technologies

measurement, in particular, is a fundamental parameter in SHM, as it provides critical insight into load distribution, fatigue resistance and the long-term performance of civil structures.

A variety of sensor technologies have been employed for strain measurement in SHM, including metal foil strain gauges, fibre optic sensors and piezoelectric sensors, each with distinct advantages and limitations (Table 1). Metal foil strain gauges, which have been widely used for decades, offer precise and reliable measurements with a typical gauge factor of ~2; however, their performance is limited by adhesive degradation over time, susceptibility to environmental factors such as humidity and temperature fluctuations and challenges in long-term deployment [5, 6]. Fibre optic sensors, particularly Fibre Bragg Grating (FBG) sensors, provide high-resolution strain measurements and are immune to electromagnetic interference, making them ideal for critical infrastructure applications [7-9]. However, fibre optic technology is expensive, requires specialized interrogation systems and can be fragile in harsh environments. Piezoelectric sensors, while effective for dynamic strain and vibration measurements, require external power sources and complex signal conditioning, making them less suitable for long-term static strain monitoring [10-12].

Table 1 - Comparative Analysis of Strain Sensing Technologies for Structural Health Monitoring (SHM) [13-15].

Technology	Metal Foil	Fiber Optic	Piezoelectric	Thick-Film
Gauge Factor (GF)	~2	0.8–1.2	Varies (depends on material)	2–35 (depends on composition)
TCR (ppm/°C)	±5 to ±20	~0	Varies (can be high)	±50 to ±200
Durability	High (if well bonded)	Very high	Moderate	Very high
Environmental Stability	Moderate (affected by humidity and adhesive degradation)	Excellent (immune to electromagnetic interference, resistant to temperature/humidity)	Moderate (sensitive to temperature fluctuations)	High (temperature stable, resistant to mechanical wear)
Cost	Low	High	Moderate to high	Low to moderate
Ease of Integration	Moderate	Complex (requires optical interrogation)	Complex (requires external power and signal conditioning)	High (can be screen-printed and mass-produced)
Response Time	Fast (milliseconds)	Fast (microseconds)	Fast (microseconds)	Fast (milliseconds)
Sensitivity to Noise	Moderate (susceptible to electromagnetic interference)	Very Low (immune to electromagnetic interference)	Low (can be affected by environmental vibrations)	Moderate (depends on material composition)
Advantages	Cost-effective, well-established, precise	High precision, immune to electromagnetic interference and long lifespan	Suitable for dynamic strain/vibration monitoring, high sensitivity	Robust, cost-effective, stable over time, suitable for steel structures, scalable for large-scale SHM
Limitations	Adhesive deterioration over time, limited temperature stability	Expensive, fragile, requires specialized equipment	Needs a power supply, unsuitable for long-term static strain monitoring	Substrate dependency, limited high-frequency response
Application Examples	Bridge monitoring, structural reinforcement monitoring	Long-span bridges, tunnels and dams	Vibration monitoring, earthquake detection, impact sensing	Structural health monitoring in steel bridges, high-rise buildings and railways

Thick-film strain sensors have emerged as a robust and cost-effective alternative for SHM applications, offering a unique combination of mechanical durability, environmental stability and ease of integration [16-18]. Unlike conventional strain gauges that rely on adhesive bonding, thick-film sensors utilize screen-printed resistive films that are sintered onto ceramic substrates, ensuring superior adhesion, long-term reliability and resistance to mechanical fatigue. These sensors demonstrate excellent temperature stability, with minimal resistance variation over a wide range of operating conditions, making them

well-suited for outdoor civil structures exposed to fluctuating environmental temperatures. Furthermore, thick-film strain sensors are capable of withstanding high-voltage surges, which is crucial for infrastructure elements such as bridges and high-rise buildings that are vulnerable to lightning strikes.

One of the key advantages of thick-film strain sensors is their compatibility with steel constructions, which form the backbone of modern civil engineering. Steel bars, commonly used as reinforcement in concrete structures or as standalone load-bearing elements in bridges, high-rise buildings and tunnels, require precise strain monitoring to ensure their structural integrity [19, 20]. The mechanical properties of thick-film ceramic sensors, particularly those based on $Bi_2Ru_2O_7$ resistive compositions, are well-matched with the modulus of elasticity of steel (210 GPa [21]), enabling accurate strain measurements without introducing significant material mismatches. Additionally, screen-printed thick-film sensors on alumina substrates exhibit high mechanical strength (elasticity modulus of 300–400 GPa [22]) and are more compatible with steel than with concrete (elasticity modulus of 10–30 GPa [23]). This makes them particularly suitable for direct application on exposed steel elements in contemporary glass-steel constructions, bridges and critical infrastructure.

The manufacturing process of thick-film sensors involves screen-printing a resistive paste onto ceramic substrates, followed by a controlled sintering process that ensures stable electrical and mechanical properties. This fabrication method allows for the production of customized sensor geometries and scalable manufacturing at low cost, making thick-film technology a viable alternative to traditional strain measurement solutions. Moreover, thick-film sensors can be integrated into sensor arrays using hybrid microelectronic techniques, enabling real-time monitoring of large-scale structural components with distributed sensing capabilities. These features position thick-film technology as an optimal choice for SHM, combining high precision, mechanical robustness, cost efficiency and long-term reliability in the assessment of steel structures.

This study investigates the performance of screen-printed $Bi_2Ru_2O_7$-based strain sensors applied to steel bars, evaluating their strain sensitivity, temperature stability and resistance to high-voltage surges under real-world conditions. The results demonstrate the potential of thick-film technology as a reliable and scalable solution for SHM, offering superior durability and environmental resilience compared to conventional strain measurement techniques. By integrating thick-film sensors into civil infrastructure, engineers can enhance the predictive maintenance of steel constructions, reducing maintenance costs and extending the service life of critical structures.

2 Stress-Induced Dynamics in $Bi_2Ru_2O_7$-based Strain Sensors

Piezoresistance is a commonly used term to describe the piezoresistive behavior of thick resistive films. It is quantitatively described by the gauge factor (GF), which relates mechanical strain to the resulting change in resistance:

$$GF = \frac{\Delta R/R}{\varepsilon} = \frac{\Delta R/R}{\Delta l/l} \tag{1}$$

where $\Delta R/R$ represents the relative change in resistance and ε denotes the strain along the length l of the resistive film.

For a resistive thick film of the standard rectangular geometry, the resistance is given by the well-established analytical relation:

$$R = \rho \frac{l}{S} = \rho \frac{l}{wt} \tag{2}$$

where ρ denotes the bulk resistivity, S the cross-section, w the width, and t the thickness of the resistive film. When a uniaxial strain is applied along the length of the resistor, the resulting change in resistance can be determined using the following relation:

$$\Delta R = \Delta l_x \frac{\rho}{S} + \Delta\rho \frac{l_x}{S} - \frac{l_x \rho \Delta S}{S^2} \tag{3}$$

Therefore, the relative variation of the resistance is obtained by dividing Eq. 3 by the original resistance as follows:

$$\frac{\Delta R}{R} = \frac{\Delta l_x \frac{\rho}{S} + \Delta\rho \frac{l_x}{S} - \frac{l_x \rho \Delta S}{S^2}}{\frac{l_x \rho}{S}} = \frac{\Delta l_x}{l_x} + \frac{\Delta\rho}{\rho} - \frac{\Delta S}{S} = \frac{\Delta l_x}{l_x} + \frac{\Delta\rho}{\rho} - \frac{\Delta w}{w} - \frac{\Delta t}{t} \tag{4}$$

By replacing the relative change in dimensions with Poisson's ratio ν and appropriate strain components:

$$\frac{\Delta w}{w} = -\nu \cdot \varepsilon; \qquad \frac{\Delta t}{t} = -\nu \cdot \varepsilon \tag{5}$$

the following expression is obtained:

$$\Delta R/R = \Delta\rho/\rho + \varepsilon(1 + 2\nu) \tag{6}$$

The gauge factor, as a measure of the sensitivity of a thick-film strain sensor, can be expressed mathematically as [24]:

$$GF = \frac{\Delta R/R}{\varepsilon} = \frac{\Delta R/R}{12\frac{T\bar{x}}{L^3}d}, \quad \bar{x} = \frac{L}{2}, \quad d \ll L \tag{7}$$

where T and d are the thickness and deflection of the substrate, respectively, L is the span between the fixed supports and x represents the mean position of the thick resistive film relative to the fixed end of the substrate. The condition d≪L ensures that the deflection remains small compared to the distance between the supports, which is a key assumption for the validity of the bending strain model.

For thick resistive films, the gauge factor is influenced by two contributions: the first term in Eq. 6, which reflects the piezoresistive characteristics of the material and the second term, which corresponds to geometrical effects. Lower gauge factors are typically associated with geometrical influences such as changes in the sensor's dimensions under strain, whereas higher gauge factors are often result from microstructural modifications that alter the material's conductivity during strain application.

Thick-film resistor compositions typically consist of three primary phases: (1) an organic vehicle which burns off at high temperatures during the firing process, (2) a glass phase usually based on lead borosilicate and (3) a conductive phase. The conductive phase, which predominantly governs the piezoresistive behaviour, typically consists of materials such as RuO_2 (ruthenium oxide) or complex ruthenates like bismuth ruthenate ($Bi_2Ru_2O_7$). The glass phase serves as a structural matrix, while the conductive phase facilitates the flow of electrical charge. Small amounts of additional oxides are often incorporated into the composition as stabilizers and to adjust the temperature coefficient of resistivity (TCR), thereby enhancing the material's performance across varying temperatures.

The gauge factor of thick resistive films is largely influenced by the microstructure of the material (Fig. 3, inset). Research has shown that metal-oxide particles embedded in the lead borosilicate glass during the sintering process form a complex conductive network that facilitates charge transport [25]. This network is not uniform and the conduction mechanisms include conduction through clusters of conducting particles, sintered contacts between adjacent particles and tunnelling through the insulating glass phase when the conductive particles are separated by thin layers of glass. The randomness and unevenness of the distribution of conductive and insulating phases create larger glass regions and conductive chains, significantly affecting the electrical properties of the film. The sheet resistance of the thick-film resistor is determined by these conduction mechanisms and the volume fraction of conductive particles in the film. Studies have demonstrated that higher sheet resistance in thick-film resistors correlates with greater gauge factor values [24], as the conduction mechanism becomes more dependent on tunnelling through glass barriers, a process that is highly sensitive to mechanical stress.

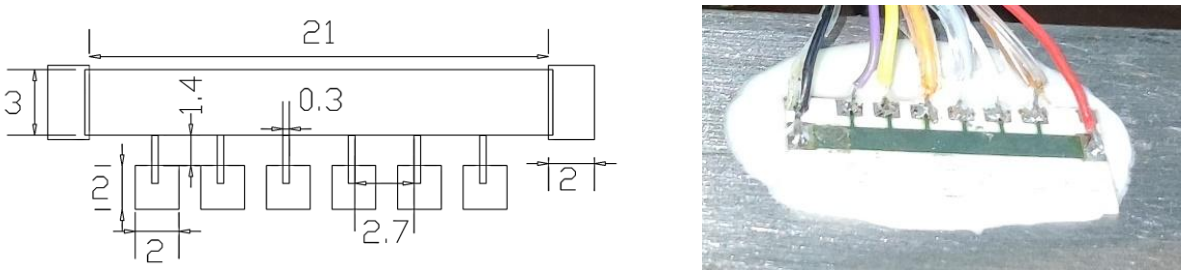
In the context of Structural Health Monitoring (SHM), an ideal strain sensor based on thick-film technology must exhibit a suitable gauge factor while being immune to external factors that may affect its performance. Among the most significant external influences are temperature fluctuations and high voltage surges. Civil engineering structures, especially those exposed to natural environmental conditions, are routinely subjected to temperature variations due to daily and seasonal changes, as well as electrical surges caused by phenomena such as lightning strikes or power grid fluctuations. These factors can alter the resistance and functionality of strain sensors if not properly addressed.

This study aims to evaluate the suitability of $Bi_2Ru_2O_7$-based strain sensors for Structural Health Monitoring, specifically focusing on their ability to operate effectively within a specified temperature range and under high voltage surge conditions. An effective strain sensor for SHM should not only exhibit a reliable gauge factor to accurately measure strain, but also maintain consistent performance under environmental stressors, such as temperature variations and voltage surges without the need for complex compensating circuitry. In this regard, the temperature stability and surge tolerance of these sensors are key parameters that will determine their viability in real-world applications, where they will be exposed to extreme environmental conditions in civil structures. Therefore, this study will assess the thermal stability of the sensors over a range of temperatures and their ability to withstand high-voltage surges, providing insights into the long-term reliability of these screen-printed $Bi_2Ru_2O_7$-based strain sensors for SHM applications.

3 $Bi_2Ru_2O_7$-Based Strain Sensors

To evaluate the application of $Bi_2Ru_2O_7$-based strain sensors on steel bars, which are commonly used in modern civil engineering, 0.635 mm thick 96% Al_2O_3 (alumina) substrates were employed. These substrates were combined with a $Bi_2Ru_2O_7$-based thick-film resistive composition, which exhibited a sheet resistance of 100 kΩ/sq. The resistive film was applied to the substrates using standard screen-printing techniques, a widely adopted method for producing thick-film sensors. This process was carried out using a semiautomatic screen printer, wherein a stainless-steel screen stretched over an aluminum frame was used to transfer the thick-film composition onto the substrate. The screen-printing process involved a squeegee moving at a constant speed, exerting consistent pressure to force the composition through the mesh of the screen, thus creating a uniform layer on the substrate surface. The printed layer pattern was defined by a 200-mesh stainless steel screen with emulsion thicknesses ranging from 10 to 12 μm, ensuring fine resolution of the printed resistive film.

A Pd/Ag conductive thick-film was utilized to fabricate contact pads on thick-film strain sensors for SHM applications. Each sensor, measuring 21×3 mm², was segmented into seven individual 3×3 mm² sections, separated by six contact pads (Fig. 1). The screen-printing process was followed by a series of controlled drying and sintering steps to ensure the formation of sensors with stable electrical properties.



(a) (b)

Fig. 1 – Thick-film strain sensor: (a) CAD drawing in mm and (b) measurement setup.

The printed resistive layers were first levelled at room temperature, followed by drying at 150 °C for 10 minutes in an infrared conveyor dryer. This drying step ensures the proper evaporation of solvents while preventing the formation of blisters, cracks, or crazing in the film. After drying, the resistive layers, which were 25 ± 3 μm in thickness, were sintered for 60 minutes, including a 10-minute dwell time at a peak temperature of 850 °C. In parallel, the conductive layers were subjected to a 30-minute sintering cycle at the same peak temperature to ensure their proper adhesion and conductivity.

The sintering process plays a key role in determining the key properties of the thick-film material, as the chemical reactions occurring in the high-temperature zone of the furnace are responsible for the final electrical and mechanical properties of the films. To guarantee uniformity and consistency, the sintering conditions were controlled throughout the process. Specifically, the airflow rates within the furnace were continuously monitored to ensure a uniform distribution of airflow across all substrates, regardless of their position on the furnace belt. The temperature control system of the furnace was calibrated to maintain precise temperature settings in each zone, which is essential for achieving uniform processing and preventing reliability issues that could affect sensor performance.

Fig. 2 depicts the temperature profile during the sintering of the thick resistive films, including the 10-minute dwell at 850 °C, measured using a thermocouple. Additionally, a Scanning Electron Microscopy (SEM) image of a fired 100 kΩ/sq $Bi_2Ru_2O_7$-based thick resistive film is shown as an inset in Fig. 2. The SEM image, captured using a JEOL JSM-35 Scanning Electron Microscope at 5000× magnification, illustrates the integration of the conductive phase within the borosilicate glass matrix, demonstrating the uniform distribution of the conductive material after firing.

All test samples were fabricated at the Institute for Electronics and Telecommunications IRITEL a.d., Belgrade, Serbia. Resistance measurements of the thick-film strain sensors were performed using the National Instruments VB-8034 Virtual Bench Instrument, ensuring precise and accurate readings. The ceramic strain sensors were systematically tested for their response to high-voltage surges with a Haefely P6T pulse generator. In addition, current noise spectra in the 10 Hz–10 kHz range were measured before and after surge testing using a Keithley Model 103A nanovolt amplifier in combination with an HP-3561B Dynamic Signal Analyzer.

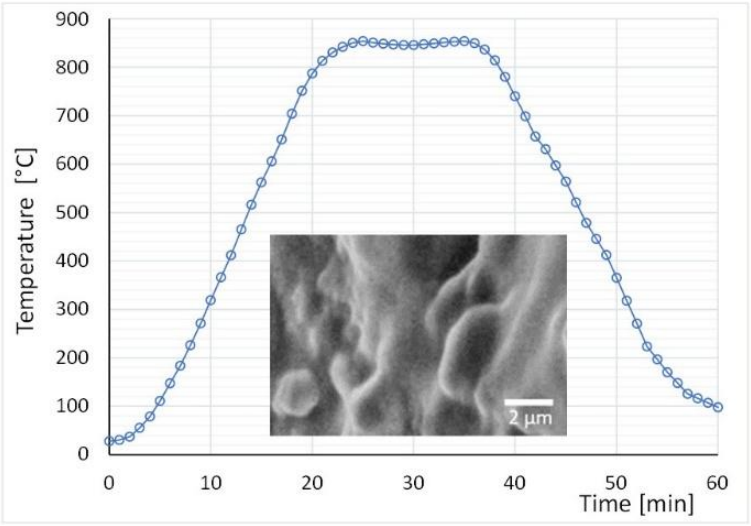
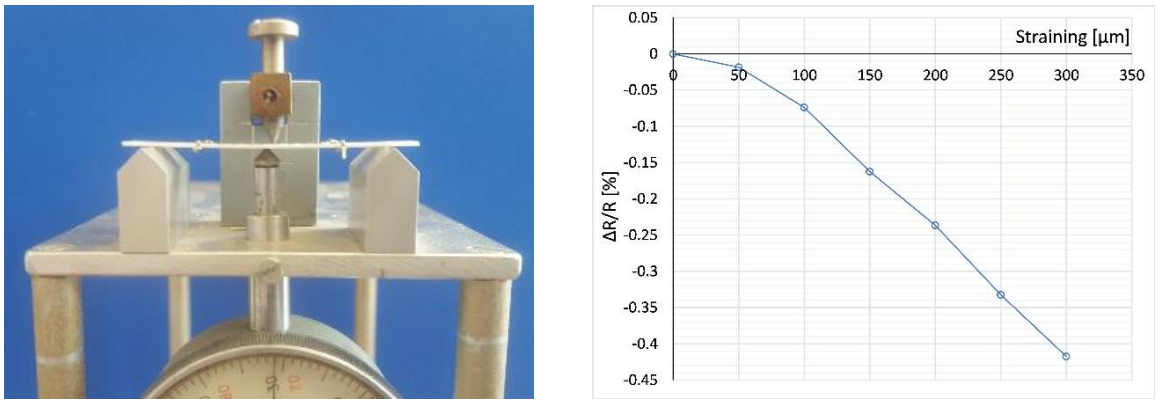


Fig. 2 – Sintering temperature profile of $Bi_2Ru_2O_7$-based thick resistive film with a 10-minute dwell at a peak temperature of 850 °C. Inset: Scanning Electron Microscopy (SEM) micrograph of a fired 100 kΩ/sq thick resistive film, captured using a JEOL JSM-35 SEM at 5000× magnification.

4 Performance of Thick-Film Strain Sensors

To assess the performance of $Bi_2Ru_2O_7$-based sensors under strain, both three-point and four-point bending tests were conducted. The three-point bending test provides data on the sensor's sensitivity and failure points, which are the main factors for ensuring the reliability and accuracy of sensors used in the monitoring of steel structures in civil engineering. In this test, the sensor's response to flexural stress is measured by applying a force at the center of the sensor while it is supported at two points. The maximum bending stress occurs directly beneath the loading anvil, where the highest strain is induced in the sensor (Fig. 3a).



(a) (b)

Fig. 3 – (a) Thick-film strain sensor under a three-point bending test and (b) response characteristics of the freestanding thick-film strain sensor under three-point bending conditions

For the test, each free-standing sensor sample was placed between two supports. A load was applied at the center of the sensor, creating a bending moment that induces strain in the sensor. During testing, the sensors were positioned face-up in compression mode, ensuring that the force was applied in a manner consistent with the typical loading conditions experienced by sensors in real-world steel beam applications.

As strain was applied to the sensors, strain-induced deformations led to changes in the resistance of the $Bi_2Ru_2O_7$-based thick resistive film. The test results showed that sensor failure occurred when the alumina substrate cracked at a deformation

of approximately 350 μm, indicating the threshold at which the sensor's structural integrity was compromised under the applied bending stress.

Fig. 3b illustrates the typical response of a thick-film strain sensor during the three-point bending test. The figure shows the change in resistance as the sensor is subjected to increasing strain, demonstrating how the sensor reacts to flexural stress and how its performance is affected as deformation progresses. The test results underscore the sensor's ability to measure strain in steel beams accurately up to a certain threshold, after which failure occurs due to the mechanical limitations of the alumina substrate.

The strain sensitivity of the thick-film strain sensor was quantitatively evaluated using the gauge factor (GF), which characterizes the relationship between the relative change in resistance and the mechanical strain experienced by the sensor (Eq. 7). For thick-film strain sensors, the typical gauge factor was found to be approximately 2, based on the response to a substrate deflection of 300 μm. This deflection produced a relative resistance change of around 0.42 %, as illustrated in Fig. 3b. This value of the gauge factor is consistent with other thick-film sensor systems, providing a reasonable measure of strain sensitivity for these sensors in the structural health monitoring (SHM) context.

To further investigate the strain sensitivity, resistance changes were also measured across three distinct segments of the sensor: between conductive pads 3 and 4, between conductive pads 2 and 5 and between conductive pads 1 and 6, corresponding to the resistive film lengths of 3 mm, 9 mm and 15 mm, respectively. For a substrate deflection of 300 μm, the observed relative resistance changes for these segments ranged from 0.2 % to 0.4 %, demonstrating the sensor's ability to detect strain across different sensor lengths, with the sensitivity generally increasing with the length of the resistive path.

The design of strain sensors in SHM applications typically involves either embedding the sensors within the structural material or bonding them to the surface of the material. The applied force may act either perpendicular or parallel to the sensor’s surface, depending on the specific application requirements. In the case of steel bars, which are often used in civil infrastructure, the screen-printed strain sensors were bonded to the surface of the bars using a two-component epoxy adhesive, similar to the bonding method employed for standard foil strain gauges. This adhesive provides a strong bond while ensuring that the strain transfer between the sensor and the substrate is efficient. For the tests conducted, the applied force was oriented perpendicular to the sensor’s surface, which is a typical loading condition for sensors in structural monitoring systems.

The four-point bending test is an essential method for evaluating the performance of thick-film strain sensors in structural health monitoring, particularly in the context of steel beams. This test is instrumental in simulating the strain distribution within a steel structure subjected to flexural loads. A four-point bending test was conducted on thick-film strain sensors adhered to steel bars at the Faculty of Civil Engineering, University of Belgrade (Fig. 4). Unlike the three-point bending test, where the maximum strain occurs at the central point, the four-point bending test applies maximum flexural stress between two loading points, leading to a more uniform strain distribution over the length of the specimen. This configuration is particularly advantageous for SHM of steel beams, as it closely mimics the real-world distribution of strain in structural elements.



(a) (b)

Fig. 4 – Thick-film strain sensor undergoing a four-point bending test: (a) detailed close-up and (b) complete setup view.

As shown in Fig. 5, the test demonstrated that the maximum observed change in resistance of the sensor was 0.17 %. This change reflects the sensor's sensitivity to strain under the applied loading conditions. The results indicate that the sensor, when adhered to a steel substrate, can reliably measure strain even under significant flexural stress. A key benefit of the four-point bending test is the uniform strain distribution, which enhances the accuracy of strain measurements in areas where the sensors are adhered to the steel bars. This makes the four-point bending configuration more representative of the actual strain experienced by sensors embedded in structural beams in real-world applications.

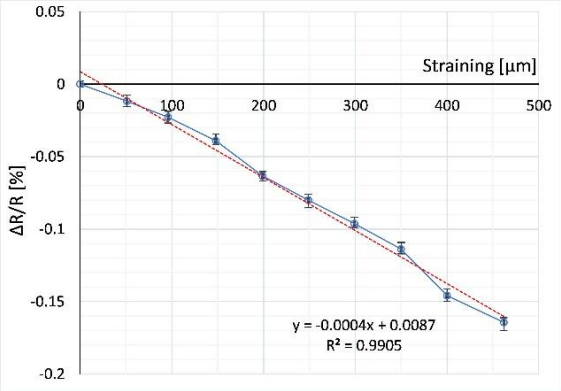
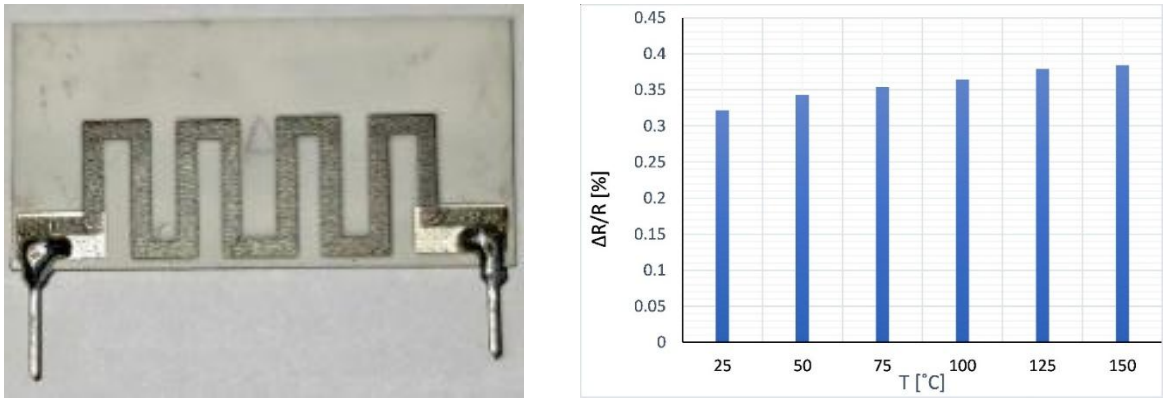


Fig. 5 – Response characteristics of thick-film strain sensor under four-point bending conditions.

Additionally, the sensors demonstrated superior performance when adhered to the steel substrate as compared to their standalone application, as evidenced by the higher strain tolerance observed in the test. This underscores the effectiveness of sensor adhesion in improving the sensor's ability to endure and accurately measure strain in structural components, enhancing their applicability for long-term SHM in steel-based civil infrastructure. However, it is important to note that the gauge factor could not be precisely determined due to variations in sensor performance influenced by adhesive type and surface preparation of the steel bars, which are critical factors in ensuring effective strain transfer and sensor accuracy.

5 Temperature Stability of Thick-Film Strain Sensors

The temperature stability of thick-film strain sensors is critical for ensuring the accurate and reliable monitoring of steel beams in civil structures, where temperature fluctuations can induce strain and affect sensor readings. To evaluate the stability of the strain sensor, a heating element was screen-printed on the reverse side of the alumina substrate in a serpentine pattern using a Pd/Ag composition (Fig. 6a).



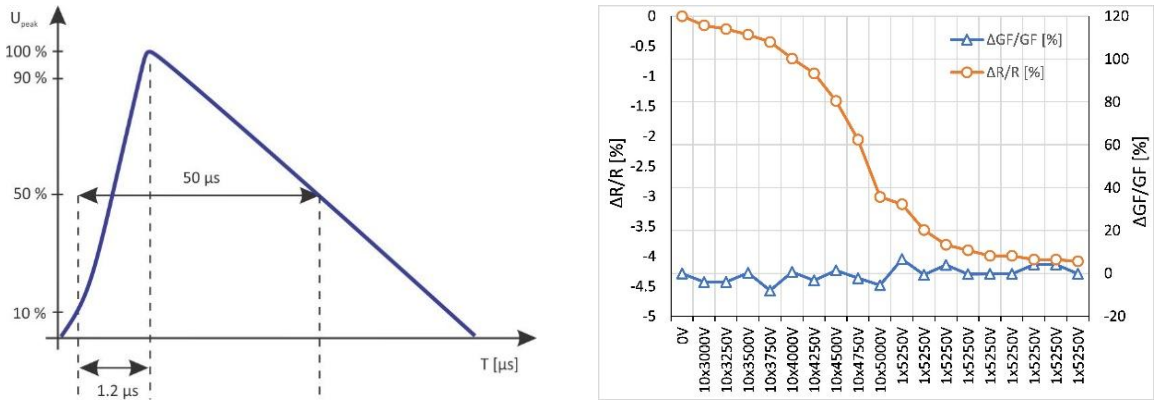
(a) (b)

Fig. 6 – Temperature Stability: (a) thick-film heating element screen-printed on the reverse side of the alumina substrate using a Pd/Ag composition and (b) temperature stability assessment of the thick-film strain sensor under a 300 μm substrate deflection across a temperature range of 25 to 150 °C.

The heater was subsequently processed following the same procedure outlined in Section 3. The temperature stability of the sensors was evaluated under 300 µm substrate deflections across a temperature range of 25 to 150 °C (Fig. 6b). The sensors exhibited excellent thermal stability, with resistance variations ranging from 0.32 % to 0.38 %, indicating minimal temperature-induced drift. Additionally, the temperature coefficient of resistance (TCR) remained nearly constant at approximately 52 ppm/°C at both 25 °C and 125 °C, demonstrating consistent sensor behavior across a broad temperature range. This stable performance is essential for accurate steel beam monitoring in civil structures, as it ensures that the strain measurements remain precise and unaffected by thermal fluctuations, thereby supporting the long-term structural health monitoring and integrity assessment of steel-based infrastructure such as bridges, buildings and other load-bearing frameworks.

6 High-Voltage Surge Evaluation of Thick-Film Strain Sensors

High-voltage surge testing is essential for evaluating the operational integrity of thick-film strain sensors used in SHM applications, particularly in steel and steel-reinforced structures. These sensors are susceptible to electrical surges arising from phenomena such as lightning strikes, power grid disturbances, or electromagnetic interference, which can lead to changes in their electrical properties or even failure [26, 27]. The performance of ceramic strain sensors under high-voltage surges was evaluated using a Haefely P6T pulse generator, which was capable of delivering 1.2/50 µs pulses to replicate fast-rising electrical transients typically encountered in structural environments (Fig. 7a). To prevent sensor detachment, a substrate deflection of 300 µm was selected, as a 460 µm deflection had been previously identified as the threshold for detachment. The electrical straining conditions were controlled to ensure a gradual, controlled variation in resistance during the pulse application. Sensors were subjected to a series of pulses with 250 V increments, spanning from 3 kV to 5.25 kV, with the generator's output resistance fixed at 25 Ω. Initially, the sensors underwent nine series of ten pulses at a frequency of six pulses per minute, starting with a pulse amplitude of 3 kV. As the pulse amplitude increased, a corresponding reduction in the sensor's resistance was observed (Fig. 7b). When resistance changes reached approximately 3 %, the pulse series was reduced to a single pulse to more accurately monitor the sensor's response to further electrical stressing. Notably, resistance values stabilized after approximately five pulses at 5.25 kV, indicating the sensor's ability to reach equilibrium under high-voltage stress. Throughout the experiment, the gauge factor values remained consistent (Fig. 7b), demonstrating that the sensor's sensitivity and functionality were preserved despite the high-voltage pulses. The electrical strain testing was conducted in full compliance with ITU-T K.20, the standard for evaluating thick-film surge resistors, ensuring the validity and relevance of the results for assessing the long-term reliability of thick-film strain sensors in structural health monitoring applications.



(a) (b)

Fig. 7 – High-Voltage Surge Test: (a) Shape of the 1.2/50 µs pulse and (b) the effect of high-voltage surges on resistance and gauge factor of the thick-film strain sensor at a substrate deflection of 300 µm.

7 Potential Application in Bridge Structural Health Monitoring

The proposed strain sensor is designed for direct measurement of structural strain responses in steel and steel-reinforced structures. It is particularly suitable for distributed deployment within structural health monitoring systems for steel bridges

[28, 29]. As illustrated in Fig. 8, sensors can be strategically installed at structurally critical locations, including mid-span regions of girders (maximum bending strain), support zones (high shear and negative bending regions), truss members subjected to axial force variations and connection details susceptible to stress concentration and fatigue damage. By continuously recording strain under operational loading conditions—including vehicular traffic, wind excitation and thermal actions—the sensor enables real-time evaluation of structural stress states based on established stress–strain relationships.

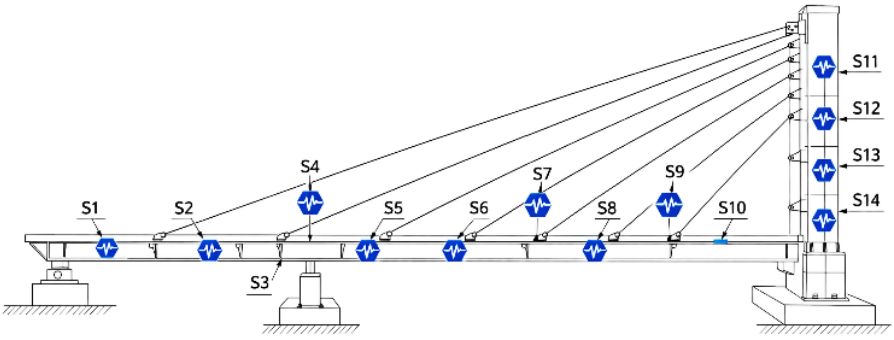


Fig. 8 – Schematic representation of distributed strain sensor locations at critical regions of a steel bridge for structural health monitoring.

Long-term strain monitoring provides insight into load redistribution, stiffness degradation and cumulative fatigue effects in steel bridge components. Variations in strain amplitude, frequency characteristics, or the accumulation of residual strain may indicate progressive damage, connection slip, or crack initiation. Compared to indirect vibration-based approaches, direct strain measurement offers higher local sensitivity to structural response, making it particularly effective for early-stage damage detection. Due to its mechanical durability under cyclic loading, thermal stability under environmental fluctuations, and stable electrical performance, the developed sensor is well-suited for long-term field deployment in bridge infrastructure. When integrated into a networked SHM framework, the sensor facilitates quantitative performance assessment, fatigue life estimation and data-driven maintenance decision-making.

8 Conclusion

This study evaluates the performance of thick-film strain sensors for structural health monitoring, specifically focusing on their application to steel bars. These sensors were fabricated on alumina ceramic substrates using a Bi2Ru2O7-based thick resistive composition and Pd/Ag conductive paste, employing established screen-printing techniques followed by controlled sintering to achieve the desired microstructural and electrical properties. The fabricated sensors underwent a series of mechanical and electrical tests to assess their reliability and performance under conditions typical of civil engineering applications.

Freestanding sensors were subjected to three-point bending tests to determine their strain sensitivity, with a calculated gauge factor of approximately 2. When mounted on steel bars, the sensors were exposed to four-point bending tests and their resistance changes were measured under varying compressive strains. The sensors demonstrated a robust mechanical performance, with resistance variations remaining below 0.17 % even under substantial deformations of up to 460 µm.

Temperature stability of the sensors was also evaluated over a range from 25 to 150 °C, revealing minimal resistance variation (between 0.32% and 0.38%) and a temperature coefficient of resistance (TCR) of 52 ppm/°C, signifying excellent thermal stability in real-world environments. Furthermore, the performance of the sensors under high-voltage surge conditions was systematically tested, with resistance values stabilizing after an initial 3% decrease, while the gauge factor remained consistent, further demonstrating the sensors' resilience to electrical transients commonly encountered in structural environments.

The combined findings of this study underscore the significant potential of thick-film strain sensors for use in SHM applications, particularly in steel and steel-reinforced structures. The sensors' ability to provide reliable strain measurements under mechanical, thermal and electrical stress, coupled with their durability and low-cost fabrication through thick-film technology, positions them as a promising alternative to traditional semiconductor-based or metal foil strain gauges. Despite

certain challenges, such as the optimization of adhesive bonding, the results of this study provide a foundation for future work that could further enhance the sensors' performance, including advancements in materials and integration strategies for large-scale SHM deployments. Moreover, the demonstrated stability under combined mechanical, thermal, and electrical loading conditions supports their suitability for long-term field deployment in structural health monitoring systems for steel and steel-reinforced structures, including bridges and other critical infrastructure. Future investigations may focus on full-scale structural implementation and long-duration in situ validation to further confirm their operational reliability in real service environments.

Acknowledgements

The authors are grateful to the Ministry of Science, Technological Development and Innovations of the Republic of Serbia (Contract No. 451-03-33/2026-03/ 200017) for the financial support.

REFERENCES

[1]- M. Ju, Z. Dou, J.W. Li, X. Qiu, B. Shen, D. Zhang, et al. Piezoelectric Materials and Sensors for Structural Health Monitoring: Fundamental Aspects, Current Status and Future Perspectives. Sensors, 23(1) (2023) 543. https://doi.org/10.3390/s23010543

[2]- A. Sofi, J.J. Regita, B. Rane, H.H. Lau, Structural health monitoring using wireless smart sensor network - An overview. Mech. Syst. Signal Process., 164 (2022) 108113. https://doi.org/10.1016/j.ymssp.2021.108113

[3]- S. Hassani, U. Dackermann, A Systematic Review of Advanced Sensor Technologies for Non-Destructive Testing and Structural Health Monitoring. Sensors, 23(4) (2023) 2204. https://doi.org/10.3390/s23042204

[4]- Z. Deng, M. Huang, N. Wan, J. Zhang, The Current Development of Structural Health Monitoring for Bridges: A Review. Buildings, 13(6) (2023) 1360. https://doi.org/10.3390/buildings13061360

[5]- R. Ottermann, E. Müller, M. Keßler, F. Dencker, D. Klaas, M.C. Wurz, Polymer-Free Batch Production and Application of Metal Foil-Based Thin-Film Strain Gauges. In: Proceedings of 2024 IEEE SENSORS, 2024 IEEE SENSORS, Kobe, Japan, 2024, pp. 1-4. https://doi.org/10.1109/SENSORS60989.2024.10784988

[6]- J.P. Wilson, R.L. McMahon, R.A. Muscat, O. Vargas, P. Vincent, Thin metal foil sensors. In: Proceedings of SPIE 6414, Smart Structures, Devices and Systems III, 2007, 64140C. https://doi.org/10.1117/12.696477

[7]- I. Dhingra, G. Kaur, R.S. Kaler, Design and analysis of fiber Bragg grating sensor to monitor strain and temperature for structural health monitoring. Opt. Quantum Electron., 53(10) (2021) 619. https://doi.org/10.1007/s11082-021-03270-7

[8]- S. Saha, S.A. Hadigheh, I. Rukhlenko, M. Valix, B. Uy, S. Fleming, et al. Machine learning-augmented multi-arrayed fiber bragg grating sensors for enhanced structural health monitoring by discriminating strain and temperature variations. J. Civ. Struct. Health Monit., 15(3) (2025) 597-618. https://doi.org/10.1007/s13349-024-00827-4

[9]- F.I. Harger Sakiyama, F. Lehmann, H. Garrecht, Structural health monitoring of concrete structures using fibre-optic-based sensors: a review. Mag. Concr. Res., 73(4) (2021) 174-194. https://doi.org/10.1680/jmacr.19.00185

[10]- D.S. Aulakh, S. Bhalla, 3D torsional experimental strain modal analysis for structural health monitoring using piezoelectric sensors. Measurement, 180 (2021) 109476. https://doi.org/10.1016/j.measurement.2021.109476

[11]- R.K. Langat, W. Deng, E. De Luycker, A. Cantarel, M. Rakotondrabe, In-situ piezoelectric sensors for structural health monitoring with machine learning integration. Mechatronics, 106 (2025) 103297. https://doi.org/10.1016/j.mechatronics.2025.103297

[12]- R. Gomasa, V. Talakokula, S.K.R. Jyosyula, T. Bansal, A review on health monitoring of concrete structures using embedded piezoelectric sensor. Constr. Build. Mater., 405 (2023) 133179. https://doi.org/10.1016/j.conbuildmat.2023.133179

[13]- B. Morten, M. Prudenziati, Piezoresistive thick-film sensors. In: Handbook of Sensors and Actuators – Thick Film Sensors. Section IV: Sensors for mechanical quantities, Elsevier Science Ltd., 1994, pp. 189-193.

[14]- K. Djordjevic, S. Galovic, M. Popovic, M. Nešic, I. Stanimirovic, Z. Stanimirovic, et al. Use Neural Network in Photoacoustic Measurement of Thermoelastic Properties of Aluminum foil. Measurement, 199 (2022) 111537. https://doi.org/10.1016/j.measurement.2022.111537

[15]- Z. Stanimirovic, I. Stanimirovic, S. Galovic, K. Djordjevic, E. Suljovrujic, Transmission pulse photoacoustic response of thin semiconductor plate. J. Appl. Phys., 133(19) (2023) 195701. https://doi.org/10.1063/5.0152714

[16]- M. Wen, X. Guan, Investigation of sensing performances of thick-film resistors sintered on fluorophlogopite glass-ceramic substrates. Sens. Actuators A Phys., 370 (2024) 115248. https://doi.org/10.1016/j.sna.2024.115248

[17]- S.A.A. Jabir, N.K. Gupta, Thick-Film Ceramic Strain Sensors for Structural Health Monitoring. IEEE Trans. Instrum. Meas., 60(11) (2011) 3669-3676. https://doi.org/10.1109/TIM.2011.2138310

[18]- S.A.A. Jabir, N.K. Gupta, Condition monitoring of the strength and stability of civil structures using thick film ceramic sensors. Measurement, 46(7) (2013) 2223-2231. https://doi.org/10.1016/j.measurement.2013.03.018

[19]- F. Tondolo, A. Cesetti, E. Matta, A. Quattrone, D. Sabia, Smart reinforcement steel bars with low-cost MEMS sensors for the structural health monitoring of RC structures. Constr. Build. Mater., 173 (2018) 740-753. https://doi.org/10.1016/j.conbuildmat.2018.04.045

[20]- C.G. Karayannis, C.E. Chalioris, G.M. Angeli, N.A. Papadopoulos, M.J. Favvata, C.P. Providakis, Experimental damage evaluation of reinforced concrete steel bars using piezoelectric sensors. Constr. Build. Mater., 105 (2016) 227-244. https://doi.org/10.1016/j.conbuildmat.2015.12.019

[21]- S. Munstermann, Y. Feng, W. Bleck, Influencing parameters on elastic modulus of steels. Can. Metall. Q., 53(3) (2014) 264–273. https://doi.org/10.1179/1879139514Y.0000000127

[22]- S.G. Yousef, J. Rodel, E.R. Fuller Jr., A. Zimmermann, B.S. El-Dasher, Microcrack Evolution in Alumina Ceramics: Experiment and Simulation. J. Am. Ceram. Soc., 88(10) (2005) 2809-2818. https://doi.org/10.1111/j.1551-2916.2005.00312.x

[23]- H. Yildirim, O. Sengul, Modulus of elasticity of substandard and normal concretes. Constr. Build. Mater., 25(4) (2011) 1645-1652. https://doi.org/10.1016/j.conbuildmat.2010.10.009

[24]- Z. Stanimirovic, M.M. Jevtic, I. Stanimirovic, Simultaneous Mechanical and Electrical Straining of Conventional Thick-Film Resistors. Microelectron. Reliab., 48(1) (2008) 59-67. https://doi.org/10.1016/j.microrel.2006.09.039

[25]- M.M. Jevtic, Z. Stanimirovic, I. Mrak, Low-Frequency Noise in Thick-Film Resistors due to Two-Step Tunnelling Process in Insulator Layer of Elemental MIM Cell. IEEE Trans. Compon. Packag. Technol., 22(1) (1999) 120-125. https://doi.org/10.1109/6144.759361

[26]- Z. Stanimirovic, I. Stanimirovic, Effects of High Voltage Pulse Trimming on Structural Properties of Thick-Film Resistors. Sci. Sintering, 49(1) (2017) 91-98. https://doi.org/10.2298/SOS1701091S

[27]- I. Stanimirovic, Z. Stanimirovic, Influence of HVP trimming on primary parameters of thick resistive films. J. Mater. Sci.: Mater. Electron., 28(11) (2017) 8002-8010. https://doi.org/10.1007/s10854-017-6504-7

[28]- Y. Mao, F. Xiao, G. Tian, Y. Xiang, Sensitivity analysis and sensor placement for damage identification of steel truss bridge. Structures, 73 (2025) 108310. https://doi.org/10.1016/j.istruc.2025.108310

[29]- P.F. Wang, Y.Q. Ni, J. Wang, Optimal sensor placement of bridge structure based on sensitivity-effective independence method. Bull. Earthquake Eng., 22(3) (2024) 1309–1357. https://doi.org/10.1007/s10518-023-01824-z